# Correlation of Vehicle Acceleration and Roadside Black Carbon Concentration

*M. Litzenberger[1], G. Dünnebeil[1], B. Cagran[2], A. Murg[3], D. Öttl[3], M. Van Poppel[4] and R. Orthofer[1]*

[1] AIT Austrian Institute of Technology GmbH, Vienna, A1220, Austria, martin.litzenberger@ait.ac.at
[2] City of Graz, Road Traffic Management Unit, A8020 Graz, Austria
[3] Province of Styria, Air Pollution Monitoring Unit, A8020 Graz, Austria
[4] VLAAMSE INSTELLING VOOR TECHNOLOGISCH ONDERZOEK N.V.  VITO, 2400 Mol, Belgium

## Introduction

When motor vehicles move during "stop-and-go" (stop/go) traffic, their fuel consumption and air pollutant emissions increase strongly compared to fluent traffic. These increases are a consequence of the higher engine loads and combustion dynamics during the acceleration of the vehicles. Currently urban traffic congestion situations are monitored using average speed (and average travel time) and traffic volume. The CARBOTRAF project has developed a real-time road side vehicle acceleration detection system based on the "smart-eye TDS" optical traffic monitoring sensor. This paper presents the results from a survey in Graz, where traffic sensors together with black carbon monitors have been installed in urban corridors near major traffic light-controlled junctions.

In past years, measurement of vehicle acceleration rates was done only by temporarily installing video equipment (Wilmink *et al*, 2009). Usually this involved offline post processing of the video data to produce the acceleration information, allowing for field surveys of only limited extend in time and locations. Therefore it has been unfeasible to regularly employ vehicle acceleration detection for real-time traffic emission assessment that may be beneficial for real time traffic- or air quality management actions. Furthermore, in Austria the use of traffic video detection that might reveal personal information such as cars' licence number plates is limited due to legal privacy constraints. Although the smart eye TDS looks like a conventional camera from the outside, the sensor does not identify individual images (as video systems do), but detects "signals of moving objects" including their size, speed and speed changes (Litzenberger *et al*., 2006).

One of the projects goals is to develop a sensor than can be regularly deployed in any urban situation to measure stop/go cycles for assessing traffic emissions. The vehicle detection and speed measurement algorithms of the smart eye TDS traffic sensor of project partner AIT have been improved to allow the detection of the acceleration state of a vehicle passing the sensor. In this work, traffic data from the TDS (vehicle counts and acceleration) and derived BC emissions are correlated with black carbon (BC) concentrations measured at nearby roadside stations.

## Traffic and Air Quality Measurement Equipment Deployed

In this project the Graz test site has been equipped with BC detectors (see *BC* in **Figure 1**) and with TDS traffic sensors (see *traffic* in Figure 1) on two major routes from the north, from highway A9 into the city centre, to measure the road side BC concentration, traffic volume and the vehicles acceleration and deceleration cycles, respectively. An additional BC sensor in the centre of the test area at distance of any major roads acts as a background sensor and is located in the station "Graz Nord" of the Styrian air quality measurement network (see $BC_{background}$ in **Figure 1**).

Traffic sensors provide data on stop/go cycles 100 m upstream of the most critical junctions. The selected distance from the junctions ensures that the acceleration (stop/go) events related to larger spillbacks from the stops lights are recorded by the measurements. The sensor devices have been mounted at a height of 8 meters above the ground on light poles situated in the middle of the four lane roads. Governed by local conditions the black carbon instruments have been installed some 200 m upstream of the traffic sensor location both on the westerly side of the road with some 3 to 5 m distance from the curb with the air intake in about 2 m above ground level. Locating the sensors at the same sides of the road ensures that wind conditions in the area affect both measurements in the same way, to allow for comparable results.

**Figure 1:** Location (left) and typical installation of the traffic sensors (middle) and BC monitors (right) in the Graz northern area.

Previous investigation shows that the smart-eye TDS sensor system can be deployed and operated in any real urban situation to measure stop/go cycles for assessing traffic emissions. The vehicle detection and speed measurement algorithms of the smart eye TDS traffic sensor allow the accurate detection of the acceleration of a passing vehicle (Litzenberger *et al.*, 2013). Although the smart eye TDS looks like a conventional camera from the outside, its unique ultra-high time resolution (1 millisecond) dynamic vision sensor chip allows the detection of vehicle relative speed changes of typically 20% and above.

In contrast to traditional CCD or CMOS imagers that encode image irradiance and produce constant data volume at a fixed frame-rate irrespective of scene activity, the sensor contains an 128×128 array of autonomous, self-signaling pixels which individually respond to relative changes in light intensity by placing their address on an asynchronous arbitrated bus with a latency of less than 100µs. Pixels that are not stimulated by a change in illumination are not triggered, hence static scenes produce no output. Because there is no pixel readout clock, no time quantization takes place at this point. The sensor operates largely independent of scene illumination, directly encodes object reflectance, and greatly reduces redundancy while preserving precise timing information. Because output bandwidth is automatically dedicated to the dynamic parts of the scene a robust detection of fast moving vehicles is achieved. The high dynamic range of the photosensitive element (>120 dB or 6 decades) makes the sensor ideal for applications under uncontrolled light conditions (Lichtsteiner *et al*, 2008).

The pixel locations in the imager array are encoded in the event data that are reflected as coordinates in the image space (i,j) by address-event-representation (AER) (*Boahen*, 2000). The scene information is transmitted event-by-event and stored to a binary data file as 16 bit addresses and corresponding time stamps with a 1 ms time resolution. This corresponds to a 1000 frames per second imaging when compared to a conventional video sensor. The traffic sensor is capable of transmitting 100 kilo events per second (keps) and more; however for a typical traffic surveillance scenario the peak data rate is not higher than 50keps. A visual reconstruction of the AER data as seen by the sensor is shown in Figure 2.

In contrast to the studies mentioned above, which make use of video equipment mounted on a high tower in 100 m above the road (Wilmink *et al*, 2009) or high time resolution GPS installed in a set of test vehicles (Hirschmann *et al.*, 2010), the presented technology offers easy integration into existing road side infrastructure and can capture vehicles under normal operation. Field investigation thereby becomes simpler to implement, and more representative of the actual traffic conditions. The processing capability of the embedded sensor system furthermore offers the possibility to implement the acceleration sensing directly in the device serving future traffic management systems to ingest live acceleration data from the road network at locations of interest.

Figure 2 shows a typical example of two vehicle trajectories in space-time representation as represented in an AER data set. The trajectories for one vehicle approaching the sensor with 100 km/h and one departing with 41 km/h are shown with i and j being the horizontal and vertical axis in image space, respectively. The AER data rate is indicated at the bottom axes of the figure in kilo events per second. The trajectory being sampled with 1 ms time resolution is transformed into world coordination based on the known optical parameters and allows to extract the speed and speed change of a vehicle with high precision. Methods and algorithms for speed and acceleration measurement from the data have been described in (Litzenberger *et al.*, 2013).

The black carbon measurement instruments are commercial Aethalometer devices types AE-31-ER and AE-22-ER of manufacturer Magee Scientific with no further modification for use the project. The device function is based on the measurement of light absorption changes of a UV and IR laser beams probing a filter tape.
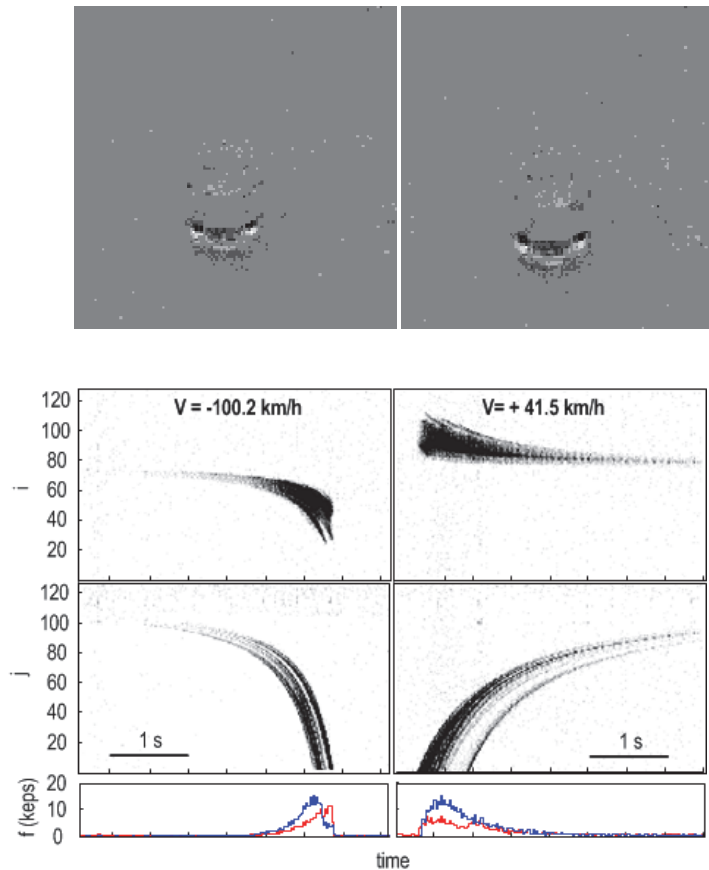


**Figure 2:** Visual representation of the smart eye TDS raw sensor data as images (two successive frames of 20 ms separation showing the front of a car) and two example vehicle trajectories in space-time representation.

## Data Acquisition System

Data of all sensors installed are acquired and stored using the openUWEDAT system of AIT Austrian Institute of Technology. The system allows flexible interfacing to multiple heterogonous data sources as use for this investigation. The data acquisition system for Graz is based on the TSAPI framework. The concept behind the TSAPI-framework is that many aspects are flexible and can be configured.

Configurable building blocks are:
- Drivers around every external device. These are called "datahandlers"
- Connections between datahandlers. They control the dataflow within the application. These connections are called "pipes".
- Intra-pipe "processors". They modify the data flow. Typical processors represent filter for invalid values, unit conversions or aggregates.
- The most convenient way to create processors is a language specialized on time series processing called "Formula3" (F3).

All building blocks and their interconnections are configurable by the use of config files. Drivers can be added to the system by a plugin concept. The TSAPI framework comes with a set of ready-made tools which are suitable for many common tasks in time series management. As they are all based on TSAPI they integrate seamlessly with each other and can be enhanced by own tools. Together they form a system that is called openUWEDAT.

The internal data concept of the TSAPI framework is based on structures that allow the definition of new fields at runtime. Thus virtually every data structure that a measurement device may emit can be handled. Different data structures can co-exist in the same system and F3 allows processing and combining them. This makes openUWEDAT and ideal system for applications that collect data from different measurement domains as it is the case in the presented work where traffic data occurs as single data sets per observed vehicle and BC measurement data are provided as time series.
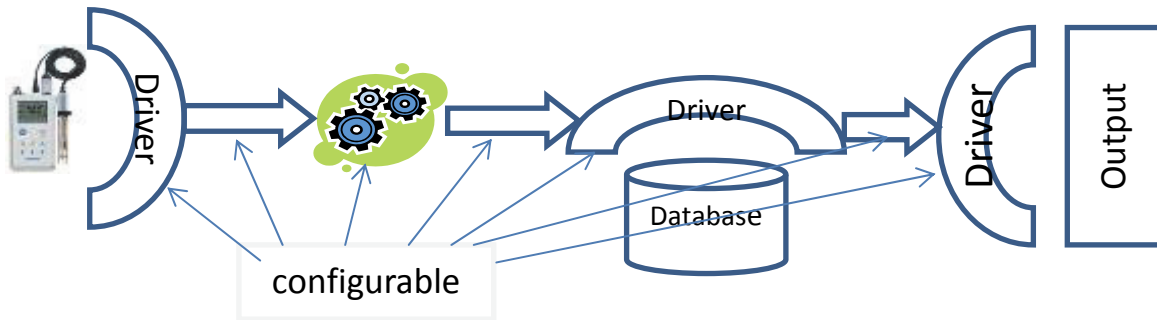


**Figure 3:** Schema of the openUWEDAT system for interfacing to multiple heterogonous data sources as used in the presented work.

## Traffic vs. local black carbon concentration

The collected traffic data are compared with BC concentrations measured at the nearby roadside stations. Figure 4 shows example data sets of daily dynamics of road side BC concentration vs. traffic flow, average speed and stop/go cycles aggregated over two lanes on two week days in November 2013.

It can be seen that the development of the stop/go cycles show a stronger similarly with the black carbon concentration curve than average speed (as another possible indicator for traffic jam) or traffic flow. The results show a coincidence of the black carbon concentration peaks with the occurrence of peaks in the acceleration events in the traffic stream. The peaks in acceleration frequency are observed during the morning and evening times accompanied only by moderate decrease in the average speed. The ration of stop/go to traffic flow is about 30% during peak traffic times and 10% during the day.

In the afternoon of the first day traffic congestion occurs, well noticeable in a sudden decrease of average speed and drop of traffic flow from 1000 veh/h to 400 veh/h. Note that there is not a distinct peak of stop/go cycles, as one might expect, because also the traffic flow rapidly decreases at the same time. However, the ratio of stop/go increases during this time from about 10% (100 /h) to 50% (200 /h) of total flow.

The following chapter details the analysis of the correlation of measured BC concentration and traffic parameters further.
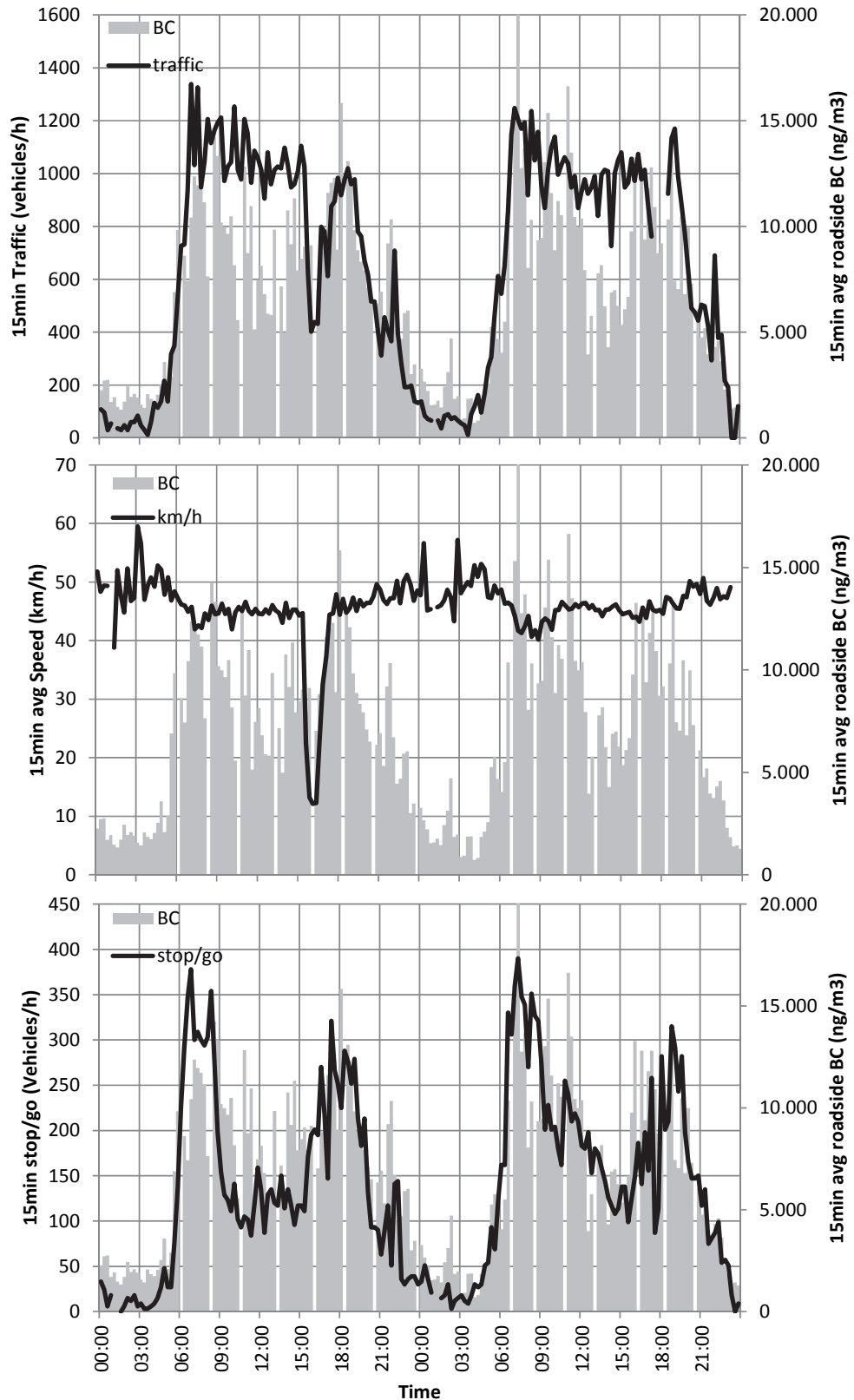
**Figure 4:** Measured roadside BC concentration versus traffic flow, average speed and stop/go cycles aggregated over two lanes on two week days.

**The Relation of vehicle BC emission strengths and BC Roadside Measurements**

A large number of scientific investigations have been conducted to measure as well as to model vehicle emissions and effect on local air quality during various stages of drive cycles and traffic dynamics (Barlow, *et al.*, 2007, Den Braven *et al.*, 2012, Hallmark *et al.*, 1999, Hirschmann *et al.*, 2010).

Smart eye TDS traffic measurement data have identified total count of vehicles as well the count of vehicles above/below an acceleration threshold of 20% of relative speed change for two categories of vehicles: class 1 = "small" (i.e. cars & motorcycles) and class 2 = "large" (i.e. light duty vehicle - LDV and heavy duty vehicle - HDV) accumulated over four lanes of traffic.

The smart eye TDS traffic data and the data from the BC sensors in the vicinity of the traffic sensors have been used to test several regression models that account for the different BC emission source strength of different vehicles categories and different acceleration situations. The underlying assumption is that (a) motor vehicle BC emissions originate mainly from Diesel exhaust, (b) that the rate of Diesel-engines in the passenger car fleet is about 55%, (c) that Diesel-powered LDV and HDV have generally much higher emissions than Diesel-powered passenger cars, (d) that emissions during stop/go movement of vehicles are much higher than during a steady flow and (e) that the rate of accelerating and decelerating vehicles is a good proxy of uneven (stop/go) traffic flow.

From the 10 models that have been tested for BC-equivalent emission strength (BC_EQUIVAL) the best fit was derived for a simple model that assumes class-2 vehicles (LDV & HDV) to have 3-fold emissions per vehicle than class-1 (mostly passenger cars). As for the influence of the traffic flow situation, the emissions strength was assumed to be 3-fold both in acceleration and deceleration status than in steady flow status (see **Table 1**). The need for including both accelerating and decelerating vehicles for higher BC-emissions is rooted in the fact that decelerating vehicles need to accelerate again at this specific measurement locations and thus influence the local BC emissions.

The model has been tested with (a) the roadside BC data that were monitored about 200 m off the traffic count locations and (b) with the roadside BC data minus the urban background BC data from the "Graz-Nord" monitoring site. As expected the "background-corrected" BC data generally had a much better fit with the BC emission strength from motor vehicles than the unadjusted BC monitoring data, the correlation between BC_EQUIVAL and background adjusted roadside BC monitoring data could be further improved when BC monitoring data during 11:00-16:00 (the time with the sunlight-induced meteorological mixing height is pronounced) were excluded from the regression analysis (see Figure 5).

**Table 1:** Emission weight factors assumed for the model of BC-equivalent emission strength used in this work.

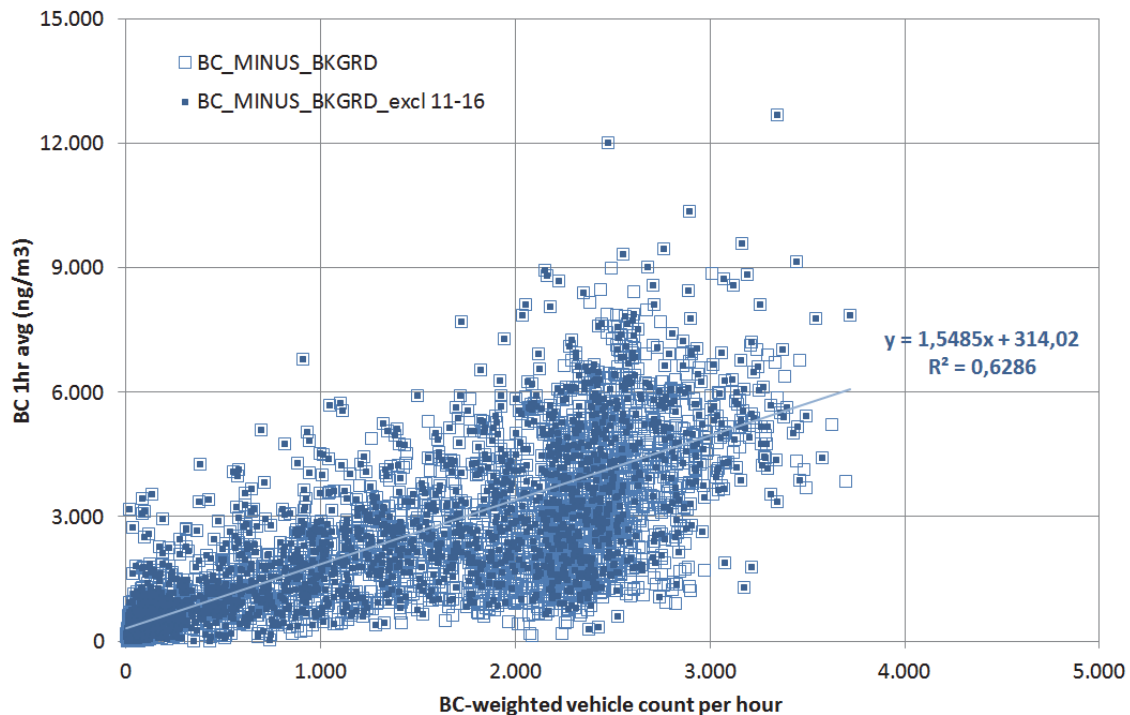|  | Steady | Accelerating | Decelerating |
| --- | --- | --- | --- |
| Class 1, Passenger cars & motor cycles | 1 | 3 | 3 |
| Class 2, LDV & HDV | 3 | 9 | 9 |

**Figure 5:** Correlation of 4006 parallel data readings of roadside 1-hr average BC concentrations and 1 hour smart eye TDS motor vehicle count weighted with BC equivalent emission strength values. Linear regression correlation is given for the data subset that excludes data monitored from 11:00 to 16:00.

## Results

Parallel monitoring of moving motor vehicle and roadside BC shows that roadside ambient BC levels are largely caused by motor vehicle emissions. The contribution of "urban background" BC levels as monitored in the Graz north station – which is influenced by non-traffic sources such as incomplete combustion of solid and liquid fuels as well as by the overall urban and suburban traffic - is relatively low throughout the year, about 2 µg/m$^3$ in winter and 1 µg/m$^3$ in summer.

The weekday temporal patterns of the roadside BC concentrations follow closely the temporal pattern of the amount of BC emission-weighted number of motor vehicles (see Figure 5). During the nights, vehicle movement and BC levels are generally very low. During all weekdays, BC concentrations increase with morning traffic up to a maximum at around 8:00 h. With decreasing traffic, BC levels decrease also. During midday, BC concentrations do not follow the traffic patterns but seem to be lower than expected from the vehicle counts. This is due to the meteorological phenomenon of generally increased atmospheric mixing during the middays. This pattern is most pronounced during weekends, when traffic generally starts later in the mornings and tend to stretch longer into the evenings. After 18:00 h, when the daytime atmospheric mixing fades, BC follows again closely the traffic counts.
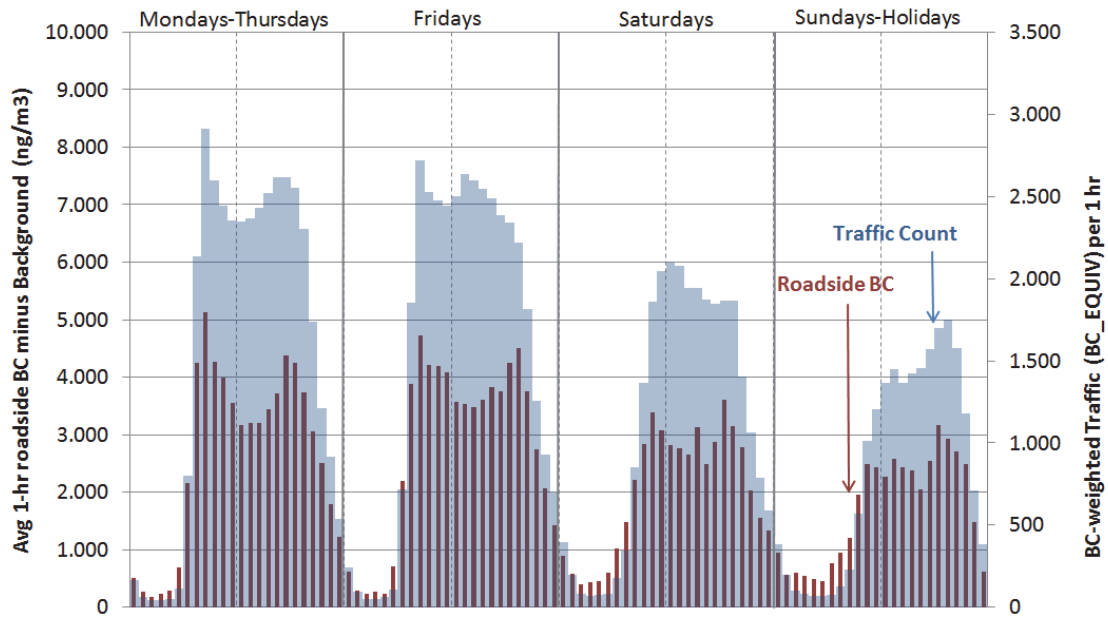
**Figure 6:** Hourly temporal dynamics of 4006 parallel data readings of roadside 1-hr average BC concentrations minus the respective urban background concentration (left y-axis) and 1-hr smart eye TDS motor vehicle counts weighted with BC equivalent emission strength values (right axis), resolved for typical weekdays.

Correlation between the average (BC-emission weighted) number of vehicles and the roadside BC-concentrations is very high (See Figure 7). It may be concluded that at the two roadside monitoring stations every 1000 motor vehicles would lead to an increase of 1 µg/m$^3$ BC in the roadside ambient air concentrations.
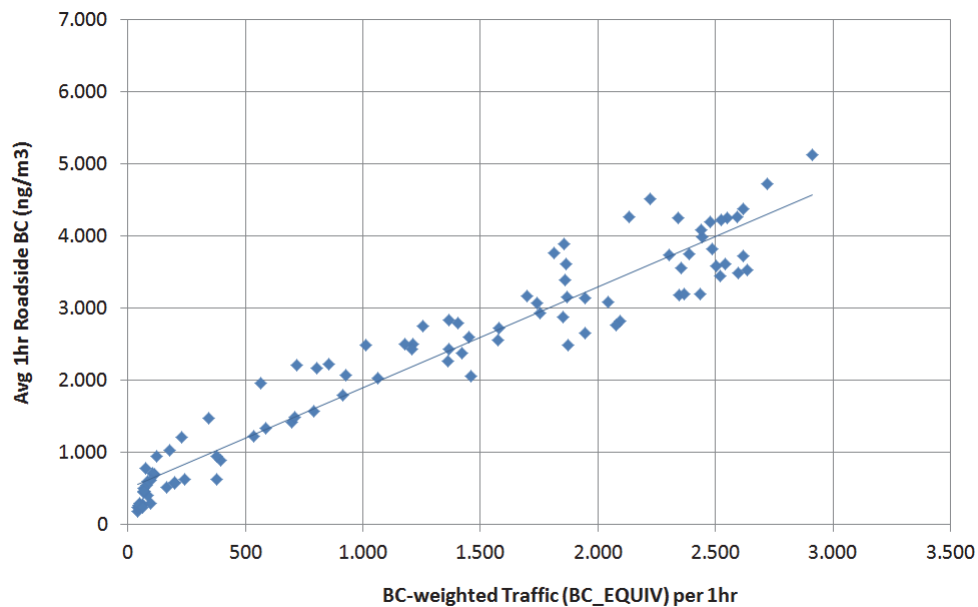


**Figure 7:** Correlation between the average (BC-emission weighted) number of vehicles and measured roadside BC-concentrations (1 hour averages).

## Conclusion

An optical sensor system has been developed than can be deployed in an urban environment to routinely measure stop/go cycles for estimating traffic induced emissions. It has been shown on data collected on major roads in the Graz urban area that a model for traffic emission source strength that takes the measured stop/go cycles into account correlates well with measured road side black carbon concentrations. In result every 1000 BC-emission weighted motor vehicles lead to an increase of 1 $\mu g/m^3$ BC in the roadside ambient air concentrations.

The results clearly demonstrate the need to routinely collect and investigate larger amounts of traffic dynamics and local air quality data to fully understand emissions and pollutant concentrations at roadside locations.

Future work in this direction will be dedicated to improve the BC emission strength model using more data under different situations, such as consideration of wind speeds and to improve the monitoring of stop/go situations through improved monitoring of vehicle acceleration status particularly during night times.

## Acknowledgement

## References

Barlow, T. J., P. G. Boulter, et al. (2007). An evaluation of instantaneous emission models, *Transport Research Laboratory. 2*.

Boahen, K. (2000), Point-to-Point Connectivity Between Neuromorphic Chips Using Address Events, *IEEE Transactions on Circuits and Systems II: Analog and Digital Signal Processing*, vol. 47 pp. 416-433, 2000.

Den Braven, K. R., A. Abdel-Rahim, et al. (2012). Modelling vehicle fuel consumption and emissions at signalized intersection approaches: Integrating field-collected data into microscopic simulation, University of Idaho.

Hallmark, S. and R. Guensler (1999). Comparison of speed-acceleration profiles from field data with NETSIM output for model air quality analysis of signalized intersections, *Transportation Research Board.*

Hirschmann, K., et al. (2010). A new method to calculate emissions with simulated traffic conditions. 13th *IEEE on Intelligent Transportation Systems*. Madeira Island, Portugal.

Lichtsteiner, P.; Posch, C.; Delbruck (2008), T., A 128×128 120dB 15us Latency Asynchronous Temporal Contrast Vision Sensor, *Solid-State Circuits, IEEE Journal of* , vol. 43, no. 2, pp. 566-576, Feb. 2008

Litzenberger M., et al., (2013) Field investigation of vehicle acceleration at the stop line with a dynamic vision sensor", *16th IEEE Conference on Intelligent Transportation Systems (ITSC 2013)*, The Hague, NL; 06.10.2013 - 09.10.2013; IEEE, 2013 (2013), Paper-No. 268

M. Litzenberger, B. Kohn, A.N. Belbachir, N. Donath, G. Gritsch, H. Garn, Ch. Posch, S. Schraml (2006) Estimation of Vehicle Speed Based on Asynchronous Data from a Silicon Retina Optical Sensor*; Intelligent Transportation Systems, 2006. Proceedings*, Toronto, CAN; 17.09.2006 - 20.09.2006; in: Intelligent Transportation Systems, 2006. Proceedings, IEEE, - (2006), ISBN: 1-4244-0094-5; S. 653 - 658.

Wilmink, I., et al. (2009) Emission Modelling at Signalised Intersections Using Microscopic Models. 16th *ITS World Congress 2009*, Stockholm, Sweden.